

Polynomial model of two interacting pacemakers taking into account the time of refractoriness

Sergey Belyakin^{1,*}, Sergey Shuteev²

¹Department of General Physics, Physics Faculty, Lomonosov Moscow State University, Moscow, Russia.

²Laboratory of dynamic systems, Physics Faculty, Lomonosov Moscow State University, Moscow, Russia.

Abstract. This publication discusses models that describe the heart tissue as an active conductive system, taking into account its self-oscillating properties. In this type of models, cardiac rhythms can be described on the basis of the theory of dynamic systems, which justifies the need to build a universal model of oscillating medium. This type of model contributes to the understanding of these pathologies cardiac activity as parasecoli and AB-blockade.

1 Introduction

The first theoretical study of cardiac arrhythmias was conducted in 1920-ies of the van - der - Pol and van - der - Mark, who proposed an electrical model of the heart [1,2]. They suggested that the activity of the heart can be simulated by three nonlinear oscillators corresponding to ACS, Atria and ventricles. This possibility was confirmed by the fact that the graphical representation of the processes occurring in the system of nonlinear oscillators had a form similar to the action potentials of heart cells. In this system, there was a unidirectional connection between the sinus and atrial oscillators, and the same connection existed between the atrial and ventricular oscillators. Reducing the connection between the latter, they found that it is possible to obtain a number of different rhythms with phase captures, qualitatively corresponding to the AB- blockades of the heart.

After the publication of the work [2], many researchers tried to model the dynamics of heartbeats, believing it to be generated by several coupled oscillators. These developments can be divided into two large groups: analysis based on continuous - time representations (ODE systems) and studies based on discrete - time representations (finite-difference equations). In this section we will consider in detail the main stages of development of these concepts and the corresponding mathematical concepts.

2 Discrete models & Of a system of interacting pacemaker

Consider some physical quantity ξ , which reflects the internal state of the biological oscillator. Let own oscillator period is equal to T_0 . Let's call a marker any event that can be clearly seen in the experiment, which is reached by the value ξ only once per period. Such a marker may be, for example, the beginning of the action potential in the cardiac preparation. Define the phase of the oscillator as follows. The phase of an arbitrarily selected marking event (for example, the maximum value of ξ) is assumed to be zero. At any next time t , $0 < t < T_0$, the phase is defined as $\varphi = t/T_0 \pmod{1}$. Since the rhythm is restored after the perturbation of the system, the introduced phase completely determines the state of the system.

Suppose that an external periodic perturbation acts on a nonlinear oscillator. Then each external influence shifts the state of the system to a new state:

$$\varphi_{n+1} = \varphi_n + f(\varphi_n) \pmod{1}. \quad (1)$$

The function $f(\varphi_n)$ is called the phase response curve (PRC) and determines the phase change after the stimulus. The points $f(\varphi_n)$ of the system state are conveniently represented lying on the circle of the unit radius. Then, by iterating the mapping (1), one point of the circle is converted to another point of the same circle. If the circle map is continuous, then it can be characterized by a number called the topological degree and equal to the number of passes φ_{n+1} on the unit circle for the time in which $f(\varphi_n)$ passes it once. In periodic perturbations of self-oscillations with a stable limit cycle, the dynamics is often described by maps of a circle with a topological degree 0 (when the over-threshold response gives rise to a new cycle) or 1 (which expresses a sub-threshold response to stimulation). The different types of circle maps are shown in fig.1.

Along with the topological degree, an important characteristic of the circle display is the number of rotations. We define it as the time average ratio of the external perturbation period to the period of the perturbed oscillator. If the rotation number is rational, $\rho = M/N$ (here M is the number of cycles of the stimulator, and N is the number of cycles of the nonlinear oscillator), then the dynamics of the system will be periodic with the capture of the phase of multiplicity N/M . If the rotation number is irrational, the system exhibits quasi-periodic or chaotic behavior.

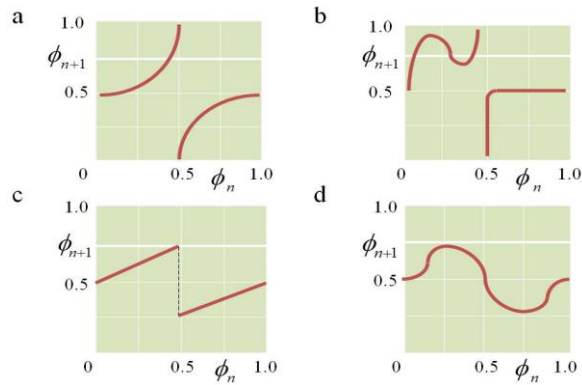


Fig.1. Different types of circle maps: (a) reversible, topological degree 1; (b) irreversible, topological degree 1; (c) piecewise continuous; (d) topological degree 0.

In many cases, the disturbance by a single pulse of a spontaneously oscillating system leads to a phase shift of the current rhythm (see, for example, [1,3] and references there). The magnitude of the shift depends on both the magnitude of the stimulus and its phase in the cycle. The graph of the dependence of the new phase on the previous phase (i.e., PRC) is either a continuous circle map with a topological degree of 1 or 0, or a discontinuous function.

Phase shift experiments have been performed for a large number of different systems. We are interested, first of all, in the phase response curve experimentally obtained in the study of a cardiac drug. In [4], the duration of the cycle of spontaneous oscillations of Purkinje fibers after stimulation with short pulses of electric current was measured. The obtained phase response curve of the biphasic form is shown in Fig. 2. Based on the study of this experimental material, the following generalizations can be made [4].

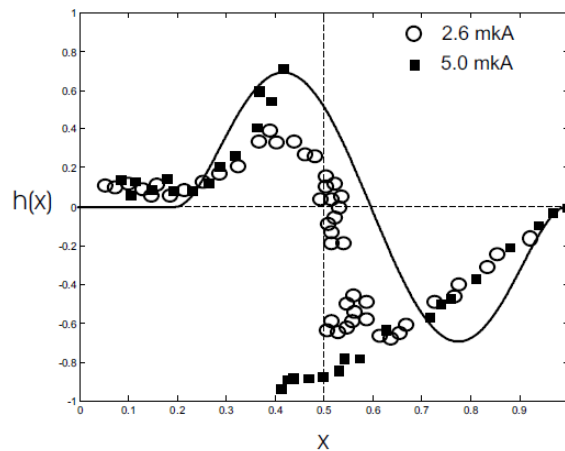


Fig.2. The phase response curve of cardiac tissue obtained experimentally [4]. The graph shows the dependence of the duration of the perturbed cycle (expressed in relative fractions of the duration of the cycle in the control) on the phase of the cycle in which the pulse is applied.

After the disturbance, the rhythm is usually restored (after a transient process) with the same frequency and amplitude as before the disturbance, and its phase is shifted. Depending on the phase, a single stimulus can either lengthen (early stimulus) or shorten (late stimulus) the duration of the perturbed cycle. At some amplitudes of the stimulus, there are obvious discontinuities.

To further study the dynamics of any constructed model, it is necessary, having experimentally obtained CFO, to find a good analytical approximation of this curve. This will allow us to investigate the main features of the behavior of the system under consideration.

The main characteristic of the desired function is the need to depend directly only on two physical parameters: the amplitude of the stimulus and the phase of the applied perturbation. All other (so-called "internal") parameters describing the course of the curve should (ideally) be reduced to the two indicated.

3 Model of two interacting pacemakers taking into account the refractoriness time

In this section, we consider two interacting leading centers (pulse oscillators) that can be pacemakers in cardiac tissue, construct a model of such interaction, and investigate its behavior.

The principle of constructing a model

Consider a system of two interacting nonlinear pulse oscillators fig.3. Let the momentum of the first oscillator with the period of undisturbed oscillations appear at the moment of time t_n , and the momentum of the second oscillator with the period of undisturbed oscillations appear at the moment τ_n . Then the moments of time of occurrence of the following pulses are defined as (2):

$$t_{n+1} = t_n + T_1, \tau_{n+1} = \tau_n + T_2. \quad (2)$$

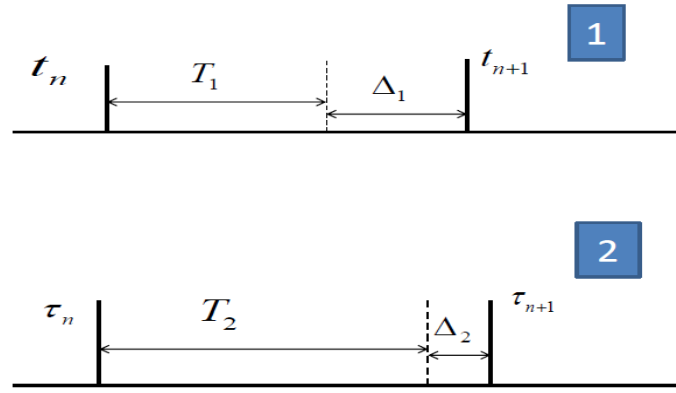


Fig.3. The scheme of construction of the model describing the system of two interacting nonlinear oscillators.

Now, assuming that under the influence of the second pulse, the period of the first oscillator will change by some value $\Delta_1((\tau_n - t_n)/T_1)$ (where the expression in parentheses shows that this value depends only on the phase of the second pulse relative to the first), then the corresponding expression for t_{n+1} will look like:

$t_{n+1} = t_n + T_1 + \Delta_1((\tau_n - t_n)/T_1)$. When you consider that $\tau_{n+1} > t_{n+1}$, that for τ_{n+1} get a similar expression: $\tau_{n+1} = \tau_n + T_2 + \Delta_2((t_{n+1} - \tau_n)/T_2)$. Dividing both of these expressions by T_1 , we find the corresponding expressions for the phases (3):

$$\begin{cases} \varphi_{n+1} = \varphi_n + \frac{1}{T_1} \Delta_1 (\delta_n - \varphi_n), \\ \delta_{n+1} = \delta_n + \frac{T_2}{T_1} + \frac{1}{T_1} \Delta_2 \left(\frac{t_n}{T_2} + \frac{T_1}{T_2} + \frac{1}{T_2} \Delta_1 (\delta_n - \varphi_n) - \frac{\tau_n}{T_2} \right). \end{cases} \quad (3)$$

Here $\varphi_n = t_n/T_1$ - phase of the first perturbed oscillator relative to the undisturbed (with the period T_1), $\delta_n = \tau_n/T_1$ - the second phase of the disturbed oscillator with respect to the same first oscillation with a period of T_1 . Introducing the parameter $a = T_2/T_1$ (the ratio of the eigenfrequencies of both oscillators) and labeling $f_1 = \Delta_1/T_1$, $f_2 = \Delta_2/T_1$, after the transformations we obtain (4):

$$\begin{cases} \varphi_{n+1} = \varphi_n + f_1 (\delta_n - \varphi_n), \\ \delta_{n+1} = \delta_n + a + f_2 \left(\frac{1}{a} (\varphi_n + 1 + f_1 (\delta_n - \varphi_n) - \delta_n) \right). \end{cases} \quad (4)$$

Since we are interested in the phase difference of the described oscillators, the final expression, which will be used in the future, is as follows (5):

$$x_{n+1} = x_n + a + f_2[(1/2)(1 + f_1(x_n) - x_n)] - f_1(x_n) \pmod{1}, \quad (5)$$

where $x_{n+1} = \delta_n - \varphi_n$.

Expression $g(x_n) = x_n + a + f_1(x_n)$, included in the right side of the equation is a circle map describing the effect of the constant perturbation on the nonlinear oscillator. Taking into account the mutual influence of oscillators leads to the appearance of an additional nonlinear term. Thus: $x_{n+1} = g(x_n) + f_2[a^{-1}(1 - g(x_n))] \pmod{1}$.

Function $f_1(x)$, $f_2(x)$ called phase response curves, which generally do not coincide with each other. Both oscillators are sources of action potentials in the same tissue, have a similar nature, and can be considered functions $f_1(x)$ and $f_2(x)$ approximately the same.

It is known that the response of the oscillator to an external stimulus depends only on the stimulus phase of its amplitude and the PRC changes its shape when the amplitude of the external influence changes. This means that the functions that define the type of phase response curves must depend on one parameter that determines the magnitude of the amplitude. In the case of this dependence can be considered multiplicative. Then the phase response curves will be written as: $f_1(x) = \gamma h(x)$, $f_2(x) = \varepsilon h(x)$.

Where $h(x)$ – periodic function, $h(x+1) = h(x)$. Under this assumption, the formula (5) will take the form:

$$x_{n+1} = x_n + a + \varepsilon h[(1/a)(1 + \gamma h(x_n) - x_n)] - \gamma h(x_n) \pmod{1}, \quad (6)$$

Let's focus on the study of the display (6) sinusoidal functions [6 – 8].

Phase diagrams for systems with mutual influence

Let us now dwell on the case of two-way communication of two pulse systems. Suppose that the effect of the first oscillator on the second one is relatively small, $\varepsilon=0.1$. As a PRC we will take $f'_1(x) = \gamma h(x)$, $f'_2(x) = \varepsilon h(x)$. For fig.2 the corresponding phase diagram obtained as a result of numerical study is presented. It depicts for comparison the same steady grips phases ratio N:M. Here n cycles of the second oscillator account for M cycles of the first one. It is easy to see that taking into account the mutual influence of the oscillators leads to bending and splitting of the capture areas. Note also that even at small values of the amplitude of the second stimulus, the main captures are superimposed on each other. The dynamics of the system thus becomes multistable. This corresponds to the situation when the limiting behavior of the display (6) depends on the initial phase difference of the oscillators x_0 .

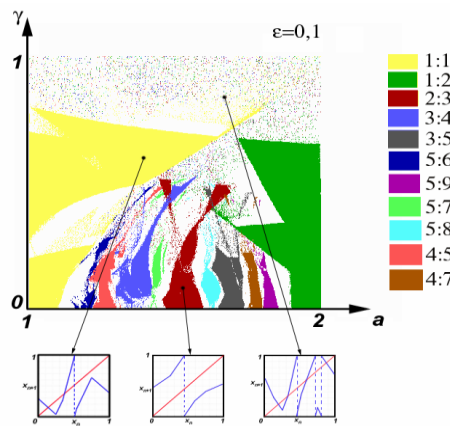


Fig.4. Areas of stable phase captures for piecewise linear mapping of a circle (2) with a PRC of the form (6) taking into account the mutual influence of oscillators.

For fig.4 the circle map (6) constructed for some values of a and γ is given. It kind of confirms that with increasing γ the system dynamics becomes more complicated, and the display ceases to be monotonous, and it appears the intervals with the slope, a large I . It can be shown [9] that for continuous circle maps this leads to multistability and chaotic dynamics.

4 Polynomial model

As another approximation of the experimental CFO we take the following polynomial function (7):

$$h(x) = Cx^2(1/2 - x)(1 - x)^2. \quad (7)$$

We choose the normalization factor C in such a way that the amplitude of $h(x)$ equals 1, i.e. $C = 20\sqrt{5}$ (see Fig.2). Then, taking into account the refractoriness, leaving the function continuous, and $\varepsilon = 0$, the map (2) will take the form (8):

$$x_{n+1} = \begin{cases} x_n + a, & 0 \leq x_n \leq \delta, \pmod{1}, \\ x_n + a + C\gamma h\left(\frac{x_n - \delta}{1 - \delta}\right), & \delta \leq x_n \leq 1, \pmod{1}, \end{cases} \quad (8)$$

where $h(x)$ is defined from (7). In contrast to the sinusoidal approximation, this curve at $x = \delta$ touches the abscissa axis. In other words, this means that the polynomial CFO, taking into account the refractoriness on the entire segment $[0; 1]$, is a smooth function. Let us now compare several cases with different values of the refractor time and the amplitude of the influence ε of the first oscillator on the second.

Change of phase diagrams with increasing refractoriness (case of one-way interaction of oscillators)

Consider the system (6,8) without taking into account the mutual influence of oscillators and the period of refractoriness (in other words, $\varepsilon = \delta = 0$), i.e. assuming in (10) $\delta = 0$. For fig.5a the regions of phase captures in parametric space (a, γ) obtained as a result of numerical investigation are presented. In this figure, the color gamut is much richer (visualization was carried out using Matlab R2007b, and the equations were solved using Microsoft Visual Studio C++ 2010 Professional (x64)). Stable phase captures up to 10:10 multiplicity captures are shown here. It can be seen that due to the smoothness of the polynomial function, the boundaries of the resonance languages blur significantly less than in the previous phase diagrams.

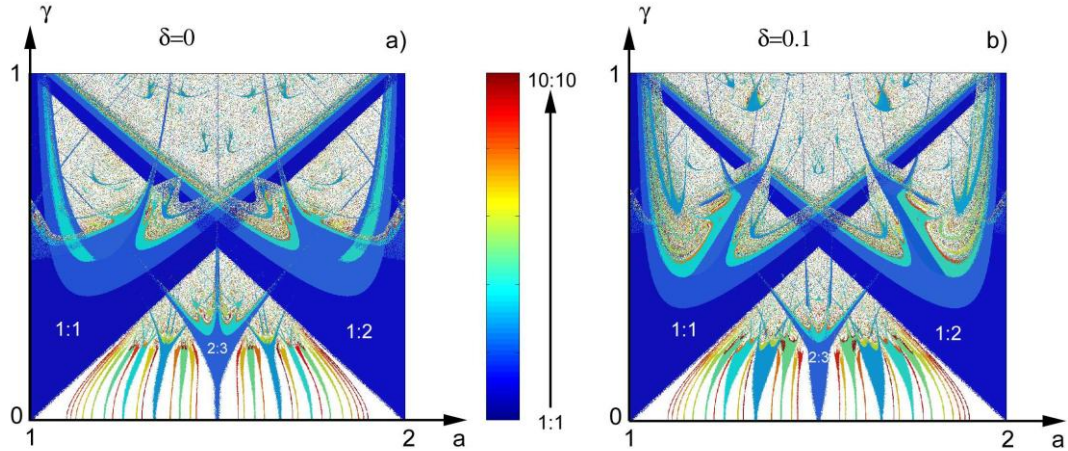


Fig.5. Phase patterns of polynomial mapping (8): (a) $\delta = 0.0$; (b) $\delta = 0.1$.

The "tails" of the main capture areas are slightly split and overlap at high temperatures. Note that, as follows from the analysis of the system (10) with $\delta = 0.1$ (Fig.5b), the introduction of refractoriness time leads to the broadening of the regions of phase captures and significant splitting and overlapping of their "tails".

For fig.6a is a numerically constructed phase diagram in the case $\delta = 0.3$. For comparison, this figure shows the same stable captures of multiplicity $N:M$ as in fig.5. It is noticeable that with an increase in refractoriness, the capture measure of the multiplicity of 2:3 increases while the measures of the main captures of 1:1 and 1:2 decrease.

The phase capture regions in the case $\delta = 0.5$ are shown in Fig.6b. This phase pattern is qualitatively different from the charts described above. The 2:3 area stretches out and looks like an arrow.

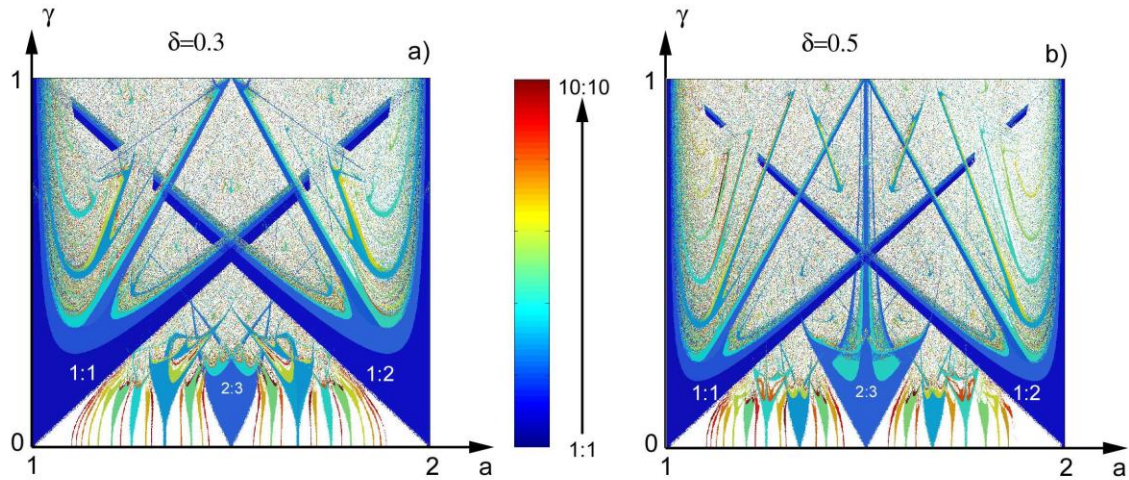


Fig.6. Phase capture regions of the display (8): (a) $\delta = 0.3$; (b) $\delta = 0.5$.

The shapes of the 3:4 and 3:5 regions also resemble arrows at $\delta = 0.7$ (Fig.7a). In the case of $\delta = 0.9$, all phase captures degenerate into vertical lines. This situation is shown in Fig.7b. note that at $\delta = 1$ there is no dependence on the amplitude of the stimulus γ (the system does not respond to external influence). In conclusion, consider the system (2) with $\delta = 0,1$ and $\varepsilon \neq 0$ in the parametric spaces (a, γ) and (ε, γ) . As an approximation function, again take (8).

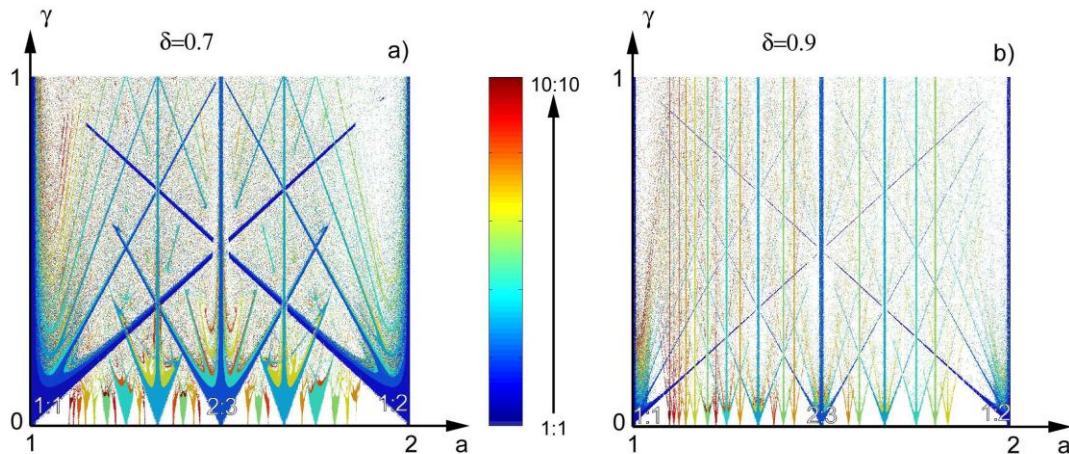


Fig.7. Phase diagrams display (8): (a) $\delta = 0.7$; (b) $\delta = 0.9$.

Phase of seizures in the space (a, γ)

Let us first assume that the effect of the first oscillator on the second is relatively small. For fig.8a the phase diagram showing the possible modes of behavior of the system of two interacting oscillators for this case is given. Mutual influence at sufficiently small values leads to similar effects, mutual influence at significantly small values leads to similar effects γ . The increase in the refractoriness time in the model with $\varepsilon = 0.1$ causes a stronger curvature of the main captures and the disappearance of the splitting regions. If we increase the value of the influence of the first oscillator to, for example, $\varepsilon = 0.5$, we see a very complex structure with a much stronger deformation of the areas of the main captures fig.8b. The 1:1 area will degenerate into a narrow strip, while the 1:2 capture area will grow due to the appearance of long narrow languages.

Numerical analysis shows that with the growth of ε to a value of ~ 0.5 , the area occupied by the resonance zones becomes larger. This leads to almost complete mixing of languages, so that it is possible to detect zones of different multiplicity in a sufficiently small neighborhood of almost any point (a, γ) . However, for these values, self-similar structures are still clearly visible. As the nonlinearity parameter ε increases further, the resonance zones decrease, taking up less and less space. In this case, there is also a very complex picture. Thus, the increase in the force of influence of the oscillators leads to mixing of the initially sufficiently ordered structure in space (a, γ) .

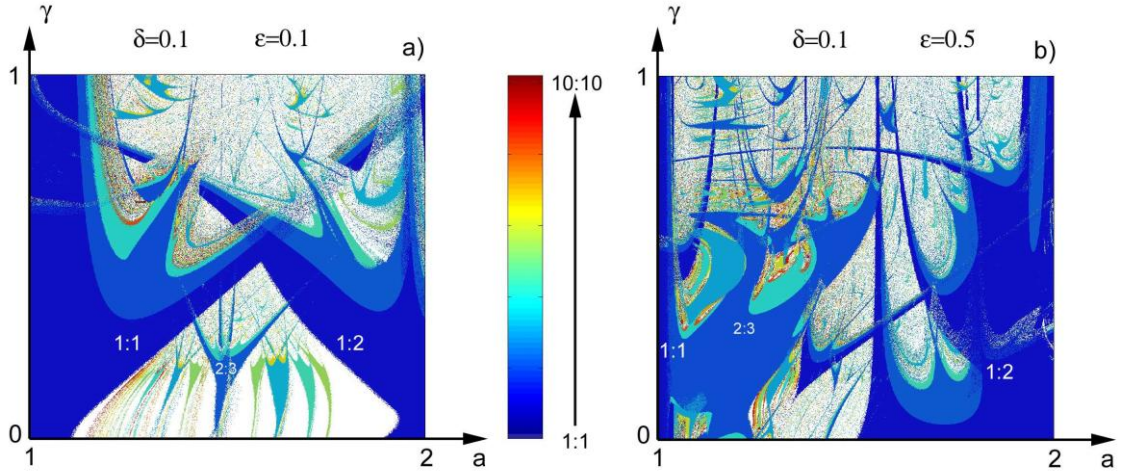


Fig.8. Phase capture areas of a system of oscillators with two-way coupling ($\delta = 0,1$): (a) $\varepsilon = 0,1$: (b) $\varepsilon = 0,5$.

The seizure phases in the space (ε, γ)

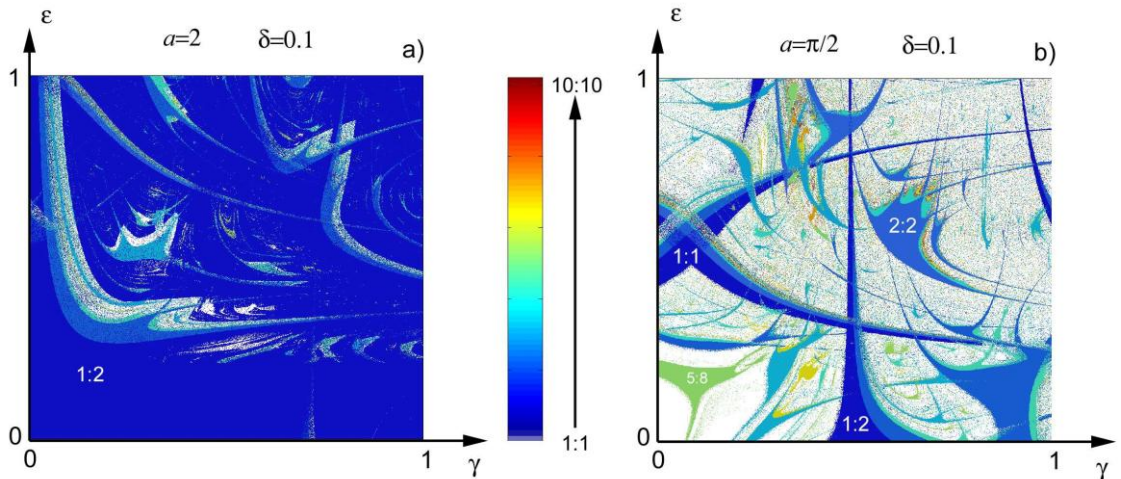


Fig.9. Phase captures in the stimulus amplitude space ($\delta = 0,1$): (a) $a = 2$: (b) $a = \pi/2$.

Let us now construct phase diagrams of interacting oscillators in the space of the influence amplitudes (ε, γ). In the first example, let $a = 2$ (fig.9a). This value of the ratio of periods means that for $\varepsilon = \gamma = 0$ the number of rotations is rational, and the dynamics of the system is periodic with a capture of $1:2$. With increasing nonlinearity, it is possible to obtain phase capture regions with a different multiplicity, even at large values of ε and γ , the periodic behavior of the system with a capture of $1:2$.

The opposite situation is observed for $a = \pi/2$. Here, the number of rotations is irrational at zero stimulus amplitudes, and the system detects a quasiperiodicity or chaotic property. With the growth of nonlinearity, there is a possibility of periodic behavior (fig.9b). In the case of sufficiently large ε , there is a decrease in the area occupied by the resonance zones. For irrational values of a , the probability of complex system behavior (8) is quite high.

5 Stabilization of complex dynamics and the possibility of full control

Any cycle of the form x_0, x_2, \dots, x_N at any $x_i \in \sigma$ is sustainable (this cycle includes a critical point), this statement allows us to practically use this method of controlling the dynamics of systems, which are effectively described by such families. Write periodically perturbed mapping explicitly:

$$\begin{cases} x_{n+1} = f(x_n, q), \\ q_{n+1} = g(q), \quad x \in M, \quad q \in Q, \end{cases} \quad (9)$$

where function f is defined by expression (10):

$$f = x + a + \varepsilon h[a^{-1}(1 + \gamma h(x) - x)] - \gamma h(x), \quad (10)$$

where a and q are parameters. The set of parameters here are a, γ, ε and δ . If the map (11) has a cycle p of period t equal to the perturbation period, $t = \tau$, $p = x_1, x_2, \dots, x_t$, the points forming this cycle will obey the following system of equations (11):

$$\begin{cases} x_2 = f(x_1, q_1), \\ x_3 = f(x_2, q_2), \\ \dots, \\ x_1 = f(x_t, q_t), \end{cases} \quad (11)$$

To solve the inverse problem, i.e. to find the parameter values at which the map (9) has a given cycle p , it is necessary to express the values from (11) q_i . It is clear that not for all possible x_i the obtained values of the parameters will satisfy the ratio $q_i \in Q$. However, if this is true for any cycle $p = x_1, x_2, \dots, x_t$ you can find the values of the parameters q_1, q_2, \dots, q_t , for which the perturbed map (9) has such a cycle.

If the multiplier of the cycle $\beta(p) = \prod_{i=1}^t f'(x_i) < 1$, it's stable. When among the points forming the cycle, there is a critical x_c , the multiplier is always less than one, which ensures stability. In case of unilateral influence of pacemakers on each other, at $\varepsilon = 0$, the display at $\gamma \geq (\sqrt{5}/5)$ for polynomial PRC taking into account refractoriness (pic.10a). The functions $f(x)$, determined from (10), under the mutual influence of oscillators are shown in (pic.10b) for polynomial PRC.

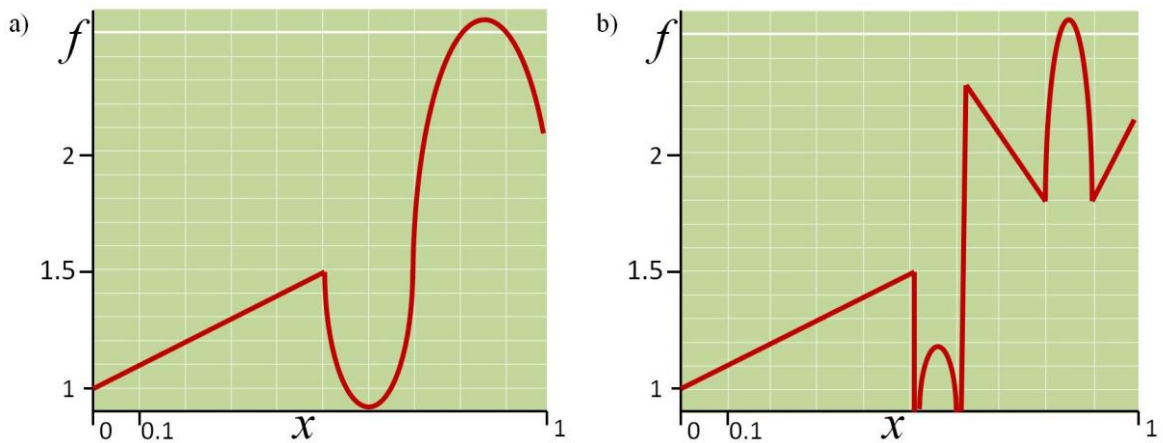


Fig.10. Functions $f(x)$ (10) at different $h(x)$ and parameter values. The ratio of periods a is fixed and is 2 (a) $h(x)$ – polynomial PRC, $\varepsilon = 0, \gamma = 0.9, \delta = 0.0$. (b) $h(x)$ is a polynomial PRC, $\varepsilon = 0.5, \gamma = 0.9, \delta = 0.5$.

Set of values $p = x_1, x_2, \dots, x_t$ for whom $q_i \in Q$ and inequality $\beta(p) = \prod_{i=1}^t f'(x_i) < 1$, forms a certain area in the coordinate space \mathbf{R} . Each point of this region corresponds to a stable cycle of disturbed mapping. Using the system of equations (11), it is possible to obtain the corresponding region in the parametric space. This enables full control of the system behavior described by the mapping (12).

From the point of view of applications to the active environment, this means that a simple parametric impact can control its dynamics. Moreover, if the behavior of the medium is chaotic, with the help of such control it is easy to stabilize it and bring the system to the required dynamic mode of motion [10].

Thus, the main result of this section is quite important for applications: for the systems described by the map (12), there are almost always such external influences, in which such systems will have a prescribed (pre-selected) dynamics.

6 Conclusion

The analogy with abnormal heart rhythms

In conclusion, we draw an analogy between the results and pathological conditions of cardiac tissue. With the help of the constructed models it is possible, for example, to describe the interaction of sinus and ectopic pacemakers, PRC and ABU, and the impact of external disturbances on the sinus rhythm. If, for example, consider the first pulse oscillator PRC, and the second – ABU, it can be found that some stable phase captures correspond to the observed pathologies in clinical practice. In this case, among the various grippers are constructed as normal sinus rhythm (capture ratio $1:1$) and classical rhythms Wenkebach (captures multiplicity $N:(N-1)$) and $N:1$ AB-blockade. If the first pulse count system of the ABU, and the second ACS, then appear inverted rhythms Wenkebach (similar to direct, but that changes the role of the ventricles and the Atria) observed in some patients.

It should be noted that the considered response functions $f_1(x) = \gamma h(x)$, $f_2(x) = \varepsilon h(x)$ for different approximations of the form, the functions $h(x)$ are model. They were taken to analyze the characteristic features of the dynamics of two nonlinear interacting oscillation sources. In practice, these functions should be chosen taking into account additional physical assumptions about the nature of the interaction and take into account the experimental data on the response of a single oscillatory system to single pulses of external perturbation. For example, in [11] the effect of short pulses on aggregates of spontaneously oscillating cells from the embryo heart was considered. The experimentally obtained phase response curves were approximated by exponential functions, and the "internal" parameters were chosen for the best correspondence of the curve graphs to the experimental points. Their dependence on physical parameters was also chosen in this way. As a result, the phase diagram obtained numerically corresponded well enough to the real dynamics of the system.

Presence of wide areas of phase captures (pic.5 – 9), in such systems, various types of synchronization of two oscillators are possible, which qualitatively correspond to some types of cardiac arrhythmias. The phase diagram allows to reveal under what conditions of interaction (i.e. at what values of parameters a , γ , ε and δ) this or that kind of synchronization is possible. Moreover, all the phase patterns presented in this paper indicate that with increasing nonlinearity (i.e., with the growth of the γ parameter), the regions with different captures begin to overlap. Knowledge of such areas and the dynamics of the system in these areas allows by external perturbation (for example, a series of single pulses) to withdraw the system from the unwanted mode of synchronization to a more favorable mode, which is vital.

Analysis of phase diagrams makes it possible to find ways to control such systems. We consider the effect of additional periodic pulse action on the behavior of interacting oscillatory subsystems. The study of possible modes of behavior of such a system by varying the frequency and amplitude of the external perturbation will lead its dynamics to a predetermined, for example, to complete suppression of the ectopic sine pacemaker. This problem, considered in the next section, is very relevant for the General theory of control of nonlinear dynamic systems and excitable media, in particular, cardiac tissue, which is satisfactorily described in the models [12,13].

7 Summary

Modern methods of removing the heart from the state of fibrillation are very rigid (supply of a short electrical pulse of a huge voltage and a large current). The development of nonlinear dynamics and synergetics made it possible to understand that such a force effect is not necessary. Often enough weak electrical effects directly on the heart muscle. Precisely, if there are spiral waves with opposite directions of rotation in the medium, then, choosing the phase and frequency of external action, it is possible to achieve the movement of the centers of the two waves towards each other and their annihilation. Now the word for careful experimental research. The theory of dynamic systems describes many processes inherent in active media, including some types of arrhythmias [1,3]. Since arrhythmias are caused by certain disorders in the heart muscle and, therefore, are pathological conditions, the modeling of such systems is of great practical interest and can bring closer to solving the problem of the possibility of controlling their behavior through external influences. This, in turn, allows us to come close to the problem of soft withdrawal of active systems from the state of developed space–time chaos that characterizes some types of pathologies [14-17]. A noteworthy work is presented in the publication [18]. In this paper, we have implemented a model of the heart, which describes the real behavior of rhythmic and arrhythmic processes in the heart.

References

1. A. Beuter, L. Glass, M.C. Mackey, *Nonlinear Dynamics in Physiology and Medicine* (New York: Springer-Verlag, Inc. 2003)
2. R.P. Grant, The mechanism of A-V arrhythmias; with an electronic analogue of the human A-V node. *Am. J. Med.* V.20. Pp.334-344 (1956)
3. R. Clayton, E. Zhuchkova, A. Panfilov, Phase singularities and filaments: Simplifying complexity in computational models of ventricular fibrillation. *Prog. Biophys. Mol. Biol.* V.90. Pp.378-398 (2006)
4. M.R. Guevara, A. Shrier, L. Glass, Phase resetting of spontaneously beating embryonic ventricular heart cell aggregates. // *Am. J. Physiol.* 1986. V.251. Pp.H1298-H1305.
5. K. Kaneko, Supercritical behavior of disordered orbits of a circle map. *Progr. Theor. Phys.* V.72. Pp.1089-1103 (1984)
6. A. Loskutov, S.D. Rybalko, E.A. Zhuchkova, A model of cardiac tissue as an excitable medium with two interacting pacemakers having a refractory time. *Banach Center Publ.* V.63. Pp.231-241 (2004)
7. A. Loskutov, S.D. Rybalko, E.A. Zhuchkova, A model of cardiac tissue as a conductive system with interacting pacemakers and refractory time. *Int. J. Bifurcation and Chaos.* V.14. Pp.2457-2466 (2004)
8. P.L. Boyland, Bifurcations of circle maps: Arnol'd tongues, bistability and rotation intervals. *Commun. Math. Phys.* V.106. Pp.353-381 (1986)
9. A. Loskutov, Nonlinear dynamics and cardiac arrhythmia, *Applied and nonlinear dynamics.* V.2. Pp.14-25 (1994)
10. A. Loskutov, S.D. Rybalko, E.A. Zhuchkova, Modeling and controlling the heart conductive system. *Proc. of the Int. Conference "Physics and Control"*. Eds. Fradkov A.L. and Churilov A.N. Saint Petersburg, Russia: *IEEE.* August 20-22, Pp.522-527 (2003)
11. L. Glass, J. Belair, D. Scagliotti, D. Gordon, A circle map in a human heart. *Physica D.* V.40. Pp.299-310 (1989)
12. M.E. Brandt, G. Chen, Controlling the dynamical behavior of a circle map model of human heart. *Biol. Cybern.* V.74. Pp.1-8 (1996)
13. D.J. Christini, J.J. Collins, Using chaos control and tracking to suppress a pathological nonchaotic rhythm in a cardiac model. *Phys. Rev. E.* V.53. Pp.R49-R52 (1996)
14. F.X. Witkowski, P.A. Penkoske, R. Plonsey, D.T. Kaplan, M.L. Spano, W.L. Ditto, K.M. Kavanagh Development of a nonlinearly deterministic signal generator for real time chaos control testing. *Eng. in Medicine and Biology Soc. IEEE 17-th Ann. Conf.* V.1. Pp.287-288 (1995)
15. M.E. Brandt, Chen Guanrong, Feedback control of a quadratic map model of cardiac chaos. *Int. J. Bifurcation and Chaos.* V.6. Pp.715-723 (1996)
16. A. Garfinkel, M.L. Spano, W.L. Ditto, Controlling cardiac chaos. *Science.* V.257. Pp.1230-1235 (1992)
17. B. van der Pol, J. van der Mark, The heartbeat considered as a relaxation oscillation and an electrical model of the heart. *Phil. Mag.* V.6. Pp.763-775 (1928)
18. Devid J. Christini, Kenneth M. Stein, Nonlinear - dynamical arrhythmia control in humans. *Medical Sciences*, vol. 98, no. 10, Pp. 5827– 5832 (2001)